

S. IMURAI*, CH. THANACHAYANONT**, J.T.H. PEARCE***, T. CHAIRUANGSRI*[#]

MICROSTRUCTURE AND EROSION-CORROSION BEHAVIOUR OF AS-CAST HIGH CHROMIUM WHITE IRONS CONTAINING MOLYBDENUM IN AQUEOUS SULFURIC-ACID SLURRY

MIKROSTRUKTURA ODLEWANYCH WYSOKOCHROMOWYCH ŻELIWI BIAŁYCH ZAWIERAJĄCYCH MOLIBDEN I ICH WŁAŚCIWOŚCI EROZYJNO-KOROZYJNE W WODNEJ ZAWIESINIE KWASU SIARKOWEGO

Microstructure and erosion-corrosion behaviour of as-cast high chromium white irons containing molybdenum in aqueous sulfuric-acid slurry was studied. The experimental irons contained 28 wt.%Cr with a Cr:C ratio of about 10 and up to 10 wt.%Mo. The irons with up to 6 wt.%Mo are hypoeutectic, whereas the iron with 10 wt.%Mo becomes eutectic/peritectic. Mo addition promotes formation of $M_{23}C_6$ and M_6C , instead of typical M_7C_3 . Erosion-corrosion testing was performed in aqueous sulfuric-acid slurry containing alumina particles. The hypoeutectic Fe-28Cr-2.7C-1Mo with mainly M_7C_3 and the eutectic/peritectic Fe-28Cr-2.6C-10Mo showed reduced wear rates of about 30% and 7% of that of the reference iron without Mo addition, respectively. The reduction of the carbide-matrix hardness difference, the increase of corrosion resistance of the matrices, and the increase of macro-hardness are determining factors for the improvement of erosion-corrosion resistance of the irons.

Keywords: high chromium cast irons, microstructure, electron microscopy, erosion, corrosion

W pracy badano mikrostrukturę odlewanych wysokochromowych żeliw białych zawierających molibden oraz ich właściwości erozyjno-korozyjne w wodnej zawieszynie kwasu siarkowego. Badane żeliwa zawierały 28% wag. chromu przy stosunku Cr:C około 10 oraz do 10% wag. molibdenu. żeliwa zawierające do 6% wag. Mo są podeutektykami, natomiast żeliwa o zawartości 10% wag. Mo – eutektykami/perytektymi. Dodatek molibdenu sprzyja powstawaniu faz $M_{23}C_6$ i M_6C , w miejsce typowego M_7C_3 . Właściwości erozyjno-korozyjne badano w wodnej zawieszynie kwasu siarkowego zawierającej cząstki tlenku glinu. Szybkość zużycia podeutektycznego żeliwa Fe-28Cr-2,7C-1Mo, zawierającego głównie M_7C_3 , oraz eutektyczny/perytektyczny Fe-28Cr-2,6C-10Mo była niższa odpowiednio o ok. 30% i 7% w odniesieniu do żeliwa bez dodatku Mo. Jako czynniki determinujące zwiększenie odporności na erozję i korozję należy wymienić: zmniejszenie różnicy twardości pomiędzy węglikiem a matrycą, wzrost odporności na korozję matrycy oraz wzrost makrotwardości.

1. Introduction

High chromium white cast irons containing 12 to 30wt%Cr and 0 to 3wt%Mo are used as cast wear parts in slurry transport, mining, minerals and cement industries [1,2]. Hypo-eutectic irons, solidifying as primary austenite dendrites followed by a eutectic mixture of austenite and M_7C_3 carbides, are mostly used [2]. Molybdenum is added to high chromium cast irons to increase hardenability but also leads to the formation of other hard carbides apart from the typical M_7C_3 , including M_2C and M_6C depending on the Cr/C ratio of the irons [3].

Wear behaviour of high chromium cast irons is complicated and depends highly on conditions during testing methodology. Hot wear resistance of Fe-20Cr-3C irons, containing up to 10 wt.%Mo and heat-treated by destabilization at 1223 K for 3 h followed by tempering at 800 K for 5 h, has been studied

by Ikeda *et al.* [4]. Dry wear testing was performed by rolling friction of two induction-heated disks at high temperature (773 K) and weight loss was measured after a controlled rolling revolution. It was found that the weight loss decreased with the increase in Mo content, because of an increase in harder eutectic M_2C instead of the typical M_7C_3 . The role of eutectic M_7C_3 and M_2C carbides on improvement of wear resistance of Mo-containing high chromium cast irons is two folds: one by resisting abrasive wear of the matrices, another by creating obstacles to the propagation of wear cracks. Liu *et al.* [5] studied dry abrasion resistance of Fe-40Cr-4.5C-8Ni-9Nb-5Mo test alloy in comparison to that of hypoeutectic Fe-25Cr-2.9C iron widely used in high temperature applications. A low stress wear tester was utilized consisting of rotating specimen holder in a stainless steel tank filled with quartz sand and an electrical furnace to heat the abrasive sand. The average wear rate of the Mo-containing test alloy was only 36% of that of the 25Cr

* DEPARTMENT OF INDUSTRIAL CHEMISTRY, CHIANG MAI UNIVERSITY, CHIANG MAI, 50200, THAILAND

** NATIONAL METAL AND MATERIALS TECHNOLOGY CENTER, PATHUMTHANI, 12120, THAILAND

*** PANYAPIWAT INSTITUTE OF MANAGEMENT, NONTHABURI, 11120, THAILAND

[#] Corresponding author: tchairuangstri@gmail.com

standard iron, indicating superior high temperature abrasion resistance. This was attributed to the hypereutectic structure of the test alloy containing primary carbide and the domination of micro-grooving and brittle fracture in wear process of the test alloy. Sliding wear behaviour of Fe-17Cr irons with up to 5 wt.%Si and 0.3 wt.% Mischmetal containing rare-earth metals has been studied by Bedolla Jacuinde and Rainforth [6]. It was concluded that the wear resistance correlated directly with the deformation depth and the depth to which carbide fracture occurred. Reduction in carbide size and connectivity by modifying alloy chemistry can minimize wear rate. Kim *et al.* [7] studied dry sand/rubber wheel abrasion wear behaviour of duo-cast materials composed of Fe-(17 to 31)Cr-(2.6 to 2.8)C irons and a low chromium steel. The Fe-17Cr-2.6C iron with eutectic carbides instead of primary carbides has better wear resistance, even though showing a lower hardness due to lower carbide volume fraction. Eutectic carbides were hardly cracked or spalled off during the wear process. In the as-cast alloys, the matrix/carbide hardness difference is large, so the matrix is selectively worn during the wear process, whereas the hardness difference is reduced in the heat-treated alloys due to austenite-to-martensite transformation and hence the wear resistance can be improved. Cardoso *et al.* [8] recently reported the wear performance of Fe-18Cr-3C-1Mo iron and some austempered ductile irons in a rotating device with an initial abrasive of 50% sand and 50% gravel.

Concerning wet conditions without corrosive media, Albertin and Sinatora [9] tested cast iron balls produced from Fe-(12 to 25)Cr-(1.6 to 3.5)C with carbide fractions of 13 to 40% by wet, ball milling with hematite (400-600 HV), phosphate rock (about 300 HV) or quartz sand (about 1000 HV) as abrasives and noted that the effect of carbide volume fraction on the wear resistance of high chromium cast irons depends on the abrasive hardness. For a very hard abrasive such as quartz, increasing the carbide volume fraction in the same metallic matrix lead to increasing wear rate by a mechanism combining rapid removal of the metallic matrix followed by micro-cracking of the carbides, consequently a martensitic steel presented the best performance against the quartz abrasive, as compared to that of high chromium cast irons. For softer abrasives such as hematite or phosphate rock, carbides can effectively protect the metallic matrix against the micro-cutting mechanism, so that wear rate decreases as the carbide volume fraction increases, up to the eutectic composition. The superior performance of austenitic cast irons in pin tests is not reproduced in the ball mill test, because low resistant matrices such as pearlite and austenite result in subsurface carbide cracking and low wear resistance in the ball mill test. Walker [10] reported wear rates of slurry pump side-liners made from Fe-27Cr-2.8C and hypereutectic Fe-30Cr against of those made from natural rubber and grey cast iron using silicious ores as abrasive. Llewellyn *et al.* [11] reported a wear ranking from the Coriolis erosion test data of several hypoeutectic and hypereutectic high chromium cast irons (up to 44% carbide volume fraction) against a standard AISI1020 steel using a slurry of silica sand (212-300 μm) as erosive medium. In this work chill cast, hypereutectic Fe-35Cr-5C iron with very fine primary carbides showed exceptionally high Coriolis erosion resistance. Stachowiak *et al.* [12] performed ball-cratering abrasion testing of Fe-25Cr-2.3C (hypoeutectic), Fe-27Cr-3C

(hypoeutectic) and Fe-30Cr-4.5C (hypereutectic) irons using large (250-300 μm) silica sand and crushed quartz slurries and a reverse wear resistance ranking as $25\text{Cr} > 27\text{Cr} > 30\text{Cr}$ was found which was completely opposite to their performance in slurry pumps in which the irons suffered from a lower stress. However, Ribeiro *et al.* [13] studied Fe-13Cr-2.6C and Fe-19Cr-2.8C irons in the as-cast condition as compared to a chilled ductile cast iron by a ball-cratering test using SiC slurry and the 19Cr iron with a higher chromium content exhibited the best wear resistance. Less information can be found for the wear behaviour of high chromium cast irons in wet conditions with corrosive media. Relative erosion-corrosion wear rate of Fe-(15 to 30)Cr-3C has been reported [14,15] and the as-cast irons with 25-30 wt.%Cr showed promising erosion-corrosion wear resistance. Gates *et al.* [16] studied synergistic corrosion-abrasion of cast wear-resistant materials in nitric acid and suggested that the Fe-15Cr-1.4C iron with an austenite matrix was the most resistant to synergistic corrosion-abrasion. Llewellyn *et al.* [11] noted that the higher Cr:C ratio in high chromium cast irons can be beneficial in certain applications where corrosion contributes significantly to overall attack.

Wear behaviour of high chromium cast irons under severe environments with erosion from hard mineral particles and also corrosion from aqueous acidic media (classified as low impact angle, low stress erosion with corrosion) is of interest. Examples of such situation are slurry-pump parts used in hydrometallurgical metal-extraction plants. Therefore, in the present work, microstructure and erosion-corrosion behaviour of as-cast Fe-28Cr-2.6C irons containing up to 10 wt.% Mo addition in aqueous sulfuric-acid slurry were studied. Details of electron microscopy of these irons have been reported elsewhere [17]. It was found that erosion-corrosion resistance increased as the Mo content in the irons increased. Determining factors responsible for the improvement of erosion-corrosion resistance of the irons include the reduction of carbide-matrix hardness difference, the increase of corrosion resistance of the matrices, and the increase of macro-hardness. The hypoeutectic and eutectic/peritectic as-cast high chromium white irons with Mo addition exhibited a promising performance in a severe erosion-corrosion environment of aqueous sulfuric-acid slurry.

2. Experimental methods

2.1. Materials

TABLE 1 shows chemical composition of the irons used in this experiment, which were cast at about 1500°C into dry sand molds as cylindrical bars with 25 mm in diameter \times 300 mm in length. They were studied in the as-cast condition.

2.2. Microstructural characterization

Microstructure of the irons was investigated by scanning electron microscopy (SEM) using a JEOL[®] 5910LV scanning electron microscope operated at 5 and 15 kV and a working distance (WD) of 10 mm. Specimens for SEM were cut from the cast cylindrical bars as 25 mm in diameter \times 15 mm height and prepared by a standard grinding and polishing procedure.

Volume fraction of microscopic constituents was determined from area fraction in SEM micrographs using the ImageJ[®] software. The average values were based on 3-10 different areas.

TABLE 1
Chemical composition of the cast irons in this experiment as analyzed by spark, atomic emission spectroscopy

Specimens	Element (wt%)									
	Fe	C	Cr	Mo	Mn	Ni	W	Si	P	S
R	Bal.	2.36	27.9	0.03	0.11	0.2	0.01	0.2	0.02	0.01
Mo1	Bal.	2.68	27.7	1.42	0.11	0.18	0.01	0.26	0.03	0.01
Mo6	Bal.	2.82	27.5	5.56	0.12	0.14	0.01	0.46	0.03	0.01
Mo10	Bal.	2.56	28.4	9.89	0.13	0.09	0.01	0.63	0.03	0.01

2.3. Hardness of the irons

Polished specimens were indented to determine Vickers macro- and micro-hardness of the irons. A Brooks[®] MAT24 macro-hardness tester (operated at 30 kgf for indentation time of 15 s) and a Galileo[®] Microscan OD V.98 micro-hardness tester (operated at 100 gf for indentation time of 15 s) were utilized. The average values were based on 10 different areas.

2.4. Erosion-corrosion testing

Specimens for erosion-corrosion tests were cut from the cast cylindrical bars as 25 mm in diameter \times 15 mm height. A erosion-corrosion testing machine designed in our laboratory was utilized. The specimens were ground down to 1,000 grit by SiC papers and mounted at an inclined angle of 15 degrees in a holder, which was then immersed in a synthetic slurry and connected to a motor rotated at a controlled speed of 500 rpm. The slurry was prepared from 2 M aqueous sulfuric acid solution mixed with alumina particles (2035 HV) with the solid-to-liquid ratio of 200 g/L. These are comparable to conditions of the slurry in hydrometallurgical zinc-extraction practice. The temperature of the aqueous acidic media was controlled during the test at 40°C by blown-air cooling. After particular testing times up to 100 h, the specimens were washed in acetone and dried. Weight loss (in g/cm²) from specimens was measured with an accuracy of 0.0001 g. The average values of weight loss were based on 3 specimens. The worn surfaces and morphology of the alumina particles were also studied by scanning electron microscopy.

3. Results and discussion

3.1. Microstructure of the experimental irons

Microstructure of the as-cast high chromium white irons in this experiment is shown in Fig. 1. The reference iron (R), the Mo1 iron, and the Mo6 iron are hypoeutectic, consisting mainly of primary dendritic austenite and eutectic (austenite+M₇C₃). Partial transformation of austenite to

martensite during cooling was also observed in the matrices. Mo promotes formation of M₂₃C₆ and M₆C, which were also found together with M₇C₃ in the Mo1 and Mo6 irons (Figs 1(b-c)). Areas where carbide transition as M₇C₃(M₂₃C) \rightarrow M₂₃C₆(M_{3.8}C) \rightarrow M₆C were also observed in SEM. At higher level of Mo addition in the Mo10 iron (Fig. 1(d)), the microstructure becomes eutectic/peritectic, containing M₂₃C₆ and M₆C without M₇C₃. Details of phase identification by electron diffraction and energy-dispersive X-ray microanalysis in transmission electron microscopy have been reported elsewhere [17].

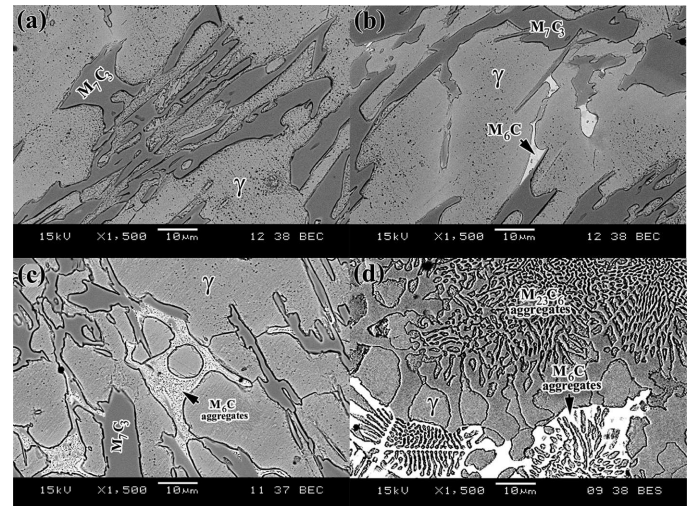


Fig. 1. Backscattered electron images in scanning electron microscope (SEM-BEI) show the microstructure of the irons: (a) the reference iron (R), (b) 1wt%Mo addition (Mo1), (c) 6wt%Mo addition (Mo6), and (d) 10wt%Mo addition (Mo10). (Etching: 1.5 g copper (II) chloride in a solution of 33 ml concentrated HCl, 33 ml absolute ethanol and 33 ml distilled water)

3.2. Metallography and hardness of the irons

The total volume fraction of carbides, the micro-hardness of dendritic austenite/martensite matrices, and the macro-hardness of the irons are given in TABLE 2. The total volume fraction of carbides in the R iron is about 37%, slightly higher than that in the Mo1 iron (33%). In Mo-containing irons, the total volume fraction of carbides increased from about 33% up to 46% as the Mo content in the irons increased from about 1 up to 10 wt.%Mo, respectively. It should be noted that this is the total volume fraction of all types of carbides, which were changed from the typical M₇C₃ to M₂₃C₆ and M₆C with increasing Mo content. The micro-hardness of dendritic austenite/martensite matrices increased only when the Mo content was less than 6 wt.%, beyond which more addition of Mo had no beneficial effect. However, overall the macro-hardness of the irons increased continuously as the Mo content was increased in the range of 1 to 10 wt.%. Even though the hardness of M₂₃C₆ (800 HV) is less than that of the M₇C₃ (1025-1500 HV), the presence of very hard M₆C (1200-1800 HV) and the hardness increase of the Mo-containing matrices cause a continuous increase of the macro-hardness of the irons.

TABLE 2

Carbide volume fraction, hardness, weight loss, and erosion-corrosion wear rate of the irons

Alloy	Phase	Volume Fraction (V_f)	Micro-Hardness ($HV_{0.1}$)	Macro-Hardness (HV_{30})	Weight Loss (g/cm^2)				Erosion-Corrosion Wear Rate ($g/(cm^2 \cdot h)$)
					1hr	10hrs	30hrs	100hrs	
R	austenite/martensite	0.63	423	495	0.0216	1.2110	2.6428	6.1314	0.064
	all carbides	0.37	NA						
Mo1	austenite/martensite	0.67	467	514	0.0024	0.4799	0.7961	1.7718	0.0187
	all carbides	0.33	NA						
Mo6	austenite/martensite	0.61	530	542	0.0017	0.3499	0.6704	1.1473	0.0126
	all carbides	0.39	NA						
Mo10	austenite/martensite	0.54	526	674	0.0009	0.1360	0.2685	0.4261	0.0047
	all carbides	0.46	NA						

3.3. Erosion-corrosion test

Morphology of the abrasive alumina particles observed from SEM is shown in Fig. 2. The agglomerate size, when the particles has not been dispersed in liquid media, is about $45 \mu m$ as shown in Fig. 2(a). However, after ultrasonic dispersing in acetone, the average particle size is about $5 \mu m$ as shown in Fig. 2(b). The average particle size after dispersion is generally less than the thickness of carbides or matrices in the irons, as compared in Fig. 1. This means that the impact by each alumina particle during erosion-corrosion test can take place on individual phases in the irons. The shape of dispersed alumina particles is platelet.

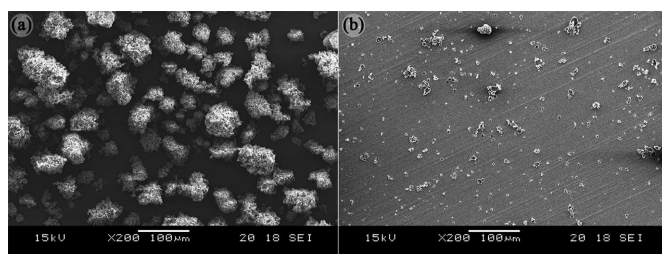


Fig. 2. Secondary electron images in scanning electron microscope (SEM-SEI) show the morphology of alumina particles: (a) before dispersion and (b) after ultrasonic dispersion in acetone

Weight loss after erosion-corrosion testing as a function of testing time given in TABLE 2 was plotted in Fig. 3(a), where a linear correlation was assumed for all cases and hence wear rates in $g/(cm^2 \cdot h)$ were determined from the slopes. Wear rates of all irons were plotted versus several factors including the Mo content (wt.%), the total volume fraction of carbides, the micro-hardness of dendritic matrices, the hardness difference between dendritic matrices and carbides, and the macro-hardness of the irons in Fig. 3(b to f), respectively. Clearly, the influence of Mo in increasing erosion-corrosion resistance is more pronounced at lower Mo content as can be seen from Fig. 3(b). By 1 wt.%Mo addition, the wear rate of the Mo1 iron was about 30% of that of the R iron without Mo addition. For the Mo content in the range of 1 to 10 wt.%, a linear correlation can be estimated between erosion-corrosion wear rate and wt.%Mo as : wear rate ($g/(cm^2 \cdot h)$) = $0.0204 - 0.00157(\text{wt.\%Mo})$. Correlations between the wear rate versus

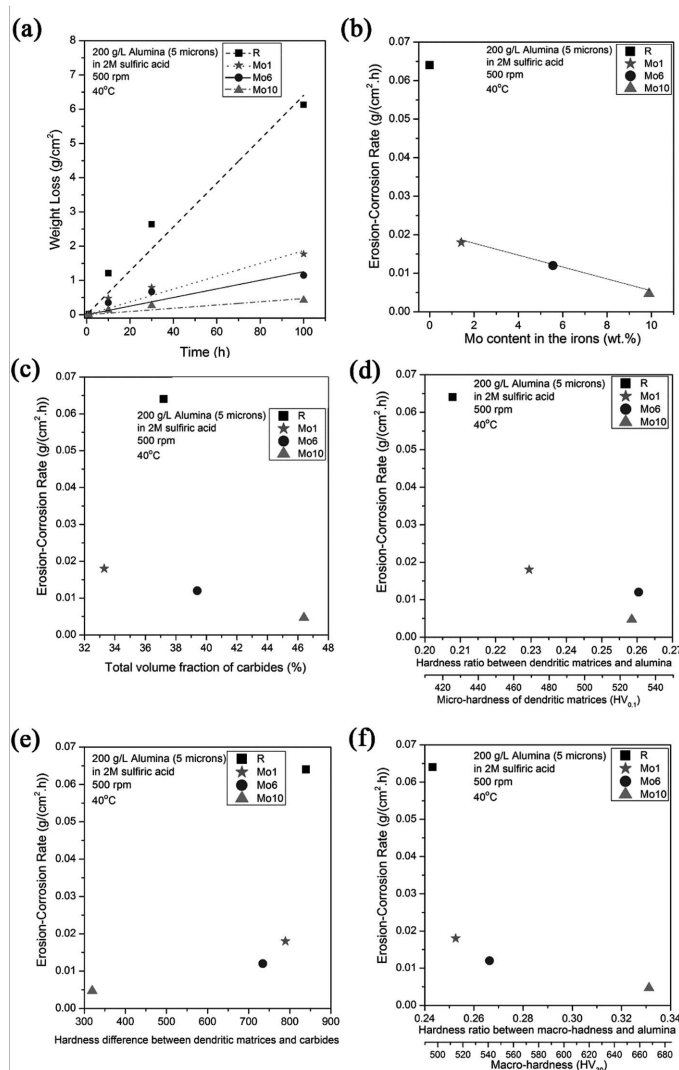


Fig. 3. (a) weight loss after erosion-corrosion testing as a function of testing time, (b to f) plots of wear rate versus the Mo content (wt.%), the total volume fraction of carbides, the micro-hardness of dendritic matrices, the hardness difference between dendritic matrices and carbides, and the macro-hardness of the irons, respectively

wt.%Mo (Fig. 3(b)), the carbide/matrix hardness difference (Fig. 3(e)) and the macro-hardness of the irons (Fig. 3(f)) show the same trend. Therefore, it can be suggested that the reduc-

tion of the carbide/matrix hardness difference, the increase of corrosion resistance of the matrices, and the increase of macro-hardness are key factors responsible for the improvement of erosion-corrosion resistance of the irons. Despite a general suggestion that the wear resistance of high chromium cast irons and carbide-containing materials should relate to the carbide volume fraction rather than the hardness of materials [15, 18], it is apparent from the results in the present study that the erosion-corrosion wear resistance of Mo-containing irons under the environment of aqueous sulfuric-acid slurry relates better to the macro-hardness of the irons than the total carbide volume fraction.

SEM micrographs of worn surfaces are shown in Fig. 4. For the reference iron, the relatively soft and low corrosion-resistant metallic matrices were rapidly worn out by micro-cutting mechanism leaving the harder eutectic M_7C_3 forming the hills, which were later cracked or spalled off. The surfaces of Mo-containing irons are more uniform, indicating a retarded wear rate of the harder and corrosion-resistant matrices and hence an effective support of the carbides by the matrices in these irons. Eutectic/peritectic carbides with less carbide spacing in the Mo10 iron effectively protected the matrices resulting in the best erosion-corrosion resistance. This agrees with the suggestions by Kim *et al.* [7] that eutectic carbides can effectively improve abrasion wear resistance and by Llewellyn *et al.* [11] that the higher Cr:C ratio can be beneficial in applications with corrosion.

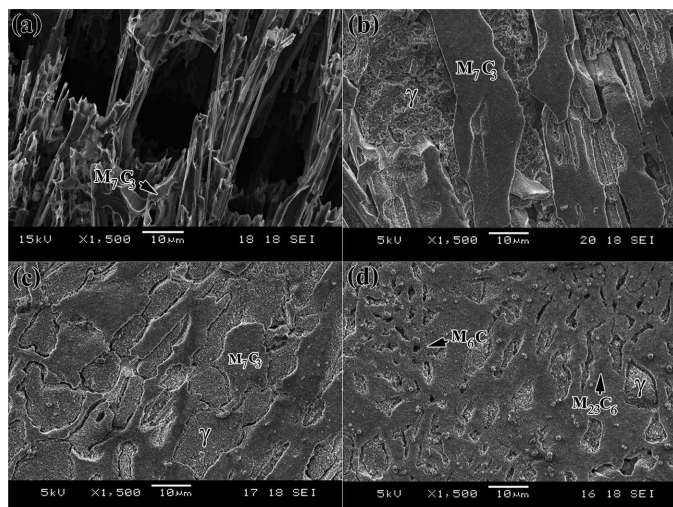


Fig. 4. Secondary electron images in scanning electron microscope (SEM-SEI) show the microstructure of worn surfaces: (a) the reference iron (R), (b) 1wt.%Mo addition (Mo1), (c) 6wt.%Mo addition (Mo6), (d) 10wt.%Mo addition (Mo10)

4. Conclusions

In the present work, the experimental as-cast Fe-28Cr white irons with the Cr:C ratios of about 10 and containing Mo up to about 6 wt.% are hypoeutectic, whereas the iron with a higher Mo addition at about 10 wt.% becomes eutectic/peritectic. Mo addition promotes formation of $M_{23}C_6$

and M_6C , instead of typical M_7C_3 . The macro-hardness of the irons increased continuously within the range of Mo addition in this study. Erosion-corrosion wear resistance under the environment of aqueous sulfuric-acid slurry increased with increasing Mo content in the irons. The hypoeutectic Fe-28Cr-2.7C-1Mo with mainly M_7C_3 and the eutectic/peritectic Fe-28Cr-2.6C-10Mo showed reduced wear rates of about 30% and 7% of that of the reference iron without Mo addition, respectively. The reduction of the carbide-matrix hardness difference, the increase of corrosion resistance of the matrices, and the increase of macro-hardness are determining factors responsible for the improvement of erosion-corrosion resistance of the irons.

Acknowledgements

The authors are grateful for the permission of accessing the electron microscopy facilities of the Electron Microscopy Research and Service Center, Faculty of science, Chiang Mai University. The Thailand Graduate Institute of Science and Technology Scholarship of the National Science and Technology Development Agency, the National Research University Project under Thailand's Office of the Higher Education Commission, and the Materials Science Research Center, Faculty of Science, Chiang Mai University are thanked for funding support.

REFERENCES

- [1] R.W. Durman, *Int. J. Miner. Process.* **22**, 381 (1988).
- [2] J.T.H. Pearce, *Foundrym.* **96**, 156 (2002).
- [3] C.P. Tabrett, I.R. Sare, M.R. Ghomashchi, *Int. Mater. Rev.* **41**, 59 (1996).
- [4] M. Ikeda, T. Umeda, C.P. Tong, T. Suzuki, N. Niwa, O. Kato, *ISIJ Inter.* **32**, 1157 (1992).
- [5] H.N. Liu, M. Sakamoto, M. Nomura, K. Ogi, *Wear* **250**, 71 (2001).
- [6] A. Bedolla Jacuinde, W.M. Rainforth, *Wear* **250**, 449 (2001).
- [7] C.Y. Kim, S. Lee, J.-Y. Jung, *Metal. Mat. Trans. A* **37A**, 633 (2006).
- [8] P.H.S. Cardoso, C.L. Israel, T.R. Strohaecker, *Wear* **313**, 29 (2014).
- [9] E. Albertin, A. Sinatora, *Wear* **250**, 492 (2001).
- [10] C.I. Walker, *Wear* **250**, 81 (2001).
- [11] R.J. Llewellyn, S.K. Yick, K.F. Dolman, *Wear* **256**, 592 (2004).
- [12] G.B. Stachowiak, G.W. Stachowiak, O. Celliers, *Trib. Int.* **38**, 1076 (2005).
- [13] L. Ribeiro, A. Barbosa, F. Viana, A. Monterio Baptista, C. Dias, C. A Ribeiro, *Wear* **270**, 535 (2011).
- [14] D.W.J. Elwell, G.M. Higginson, *World Pumps* **266**, 209-211 (1988).
- [15] J.T.H. Pearce, in: A. K. Chakrabarti, B. K. Dhindaw, J. L. Datta, C. S. Sivaramakrishnan (Ed.), *Proceedings of the 6th Asian Foundry Congress*. 120, Calcutta, India, (1999).
- [16] J.D. Gates, W.-Q. Lai, P.-S. Wen, G.A. Hope, S.A. Holt, *Cast Metals* **8**, 73-90 (1995).
- [17] S. Imurai, C. Thanachayanont, J.T.H. Pearce, K. Tsuda, T. Chairuangsi, *Mat. Charac.* **90**, 99 (2014).
- [18] T. Teker, S. Karatas, S.O. Yilmaz, *Arch. Metall. Mater.* **59**, 925, (2014).